# Estimating Seismic Demands on High-rise Concrete Shear Wall Buildings

**E. Dezhdar & P. Adebar**
*Department of Civil Engineering, The University of British Columbia, Vancouver, Canada*

**SUMMARY:**
A trilinear bending moment – curvature relationship was implemented into computer program OpenSees. Nonlinear response history analysis was conducted on 13 different buildings that were 10 to 50 stories high with a practical range of axial compression force and vertical reinforcement. Both uniform hazard spectrum (UHS) and conditional mean spectrum (CMS) were considered as target spectrum for selecting and scaling ground motions. The results from numerous nonlinear response history analyses on the 13 buildings were used to develop simplified procedures to estimate seismic demands on high-rise concrete shear wall buildings using response spectrum analysis (RSA) including: the appropriate effective stiffness values to estimate mean roof displacement, an envelope of interstory drifts over the building height, curvature demands at the base and near mid-height, and base shear force.

*Keywords: Concrete shear walls, effective stiffness, interstory drift, curvature, base shear force.*

## 1. INTRODUCTION

Concrete shear walls are extensively used as the seismic force resisting system on the west coast of North America. In order to design such buildings, estimates need to be made of the demands on the shear walls due to the design level earthquakes. While nonlinear response history analysis is sometimes used in the design of high-rise shear wall buildings in the US, linear dynamic - response spectrum - analysis is normally used to design such buildings in Canada.

In the current study, numerous nonlinear response history analyses were done on a variety of buildings in order to develop simplified procedures to estimate nonlinear demands on cantilever shear walls from linear (response spectrum) analysis. This includes: maximum wall displacement at the roof level; the complete interstory drift envelope; curvature demands at the base of cantilever walls and near mid-height where higher modes cause large bending moments, and the envelope of shear force demands.

## 2. EXAMPLE SHEAR WALL BUILDINGS

Thirteen different concrete shear wall buildings varying in height from 10 to 50 stories were included in this study (see Table 1). All buildings had the shear walls arranged in a central core with openings on two opposite sides. Thus the shear walls were coupled walls in one direction and cantilever walls in the other direction. The results are presented here for the cantilever wall direction only. All buildings with the same number of stories have the same concrete wall geometry and same mass per floor and thus same fundamental period $T_1$ based on the uncracked flexural rigidity $EI_g$. The buildings had different percentages of vertical reinforcement and different levels of axial compression in the walls due to the different placement of the gravity-load columns, and thus had different bending moment capacities at the base. The ratio $R_g$ of elastic bending moment demand (calculated using $EI_g$) to nominal bending moment capacity ranged from 1.4 to 4.4.

The vertical (longitudinal) wall reinforcement was designed according to the requirements of the Canadian Concrete Code (CSA A23.3-04). The amount of vertical reinforcement in the walls was kept constant over the plastic hinge zone (from the base to a height equal to 1.5 times the wall length) and then decreased approximately linearly over the building height. The minimum reinforcement requirements controlled the amount of reinforcement in upper levels. Cantilever walls in a core have a “C” or “I” shaped cross-section with coupled walls at each end being similar to “flanges.”

**Table 1.** Properties of Shear Wall Buildings Included in the Study.

| **No. Stories** | **10** | | | **20** | **30** | | | | **40** | **50** | | | |
|---|---|---|---|---|---|---|---|---|---|---|---|---|---|
| $L$ (m)[1] | 5.50 | | | 7.50 | 9.00 | | | | 10.75 | 13.75 | | | |
| $L_f$ (m)[2] | 6.00 | | | 8.00 | 9.00 | | | | 11.50 | 13.50 | | | |
| $L_w$ (m)[3] | 0.60 | | | 0.90 | 1.20 | | | | 1.40 | 1.60 | | | |
| $t_f$ (m)[4] | 0.45 | | | 0.55 | 0.70 | | | | 0.80 | 0.85 | | | |
| $A_g$ ($m^2$)[5] | 8.2 | | | 14.6 | 21.7 | | | | 31.2 | 42.2 | | | |
| $I_g$ ($m^4$)[6] | 39.4 | | | 126.2 | 261.4 | | | | 545.8 | 1189.5 | | | |
| $f_c'$ (MPa) | 30 | | | 35 | 40 | | | | 45 | 55 | | | |
| $E_cI_g$ ($kNm^2$) | $9.71x10^8$ | | | $3.36x10^9$ | $7.44x10^9$ | | | | $1.65x10^{10}$ | $3.78x10^{10}$ | | | |
| $m$ (kg)[7] | 825,700 | | | 927,625 | 999,000 | | | | 1,284,400 | 1,947,000 | | | |
| $T_1$ (s)[8] | 1.0 | | | 2.0 | 3.0 | | | | 4.0 | 5.0 | | | |
| $P/f_c'A_g$ (%)[9] | 5.9 | | | 8.7 | 10.1 | | | 6.1 | 6.2 | 12.7 | | | 6.2 |
| $\rho_f$ (%)[10] | 4.0 | 2.5 | 1.2 | 0.60 | 3.5 | 1.2 | 0.5 | 0.5 | 0.52 | 3.5 | 1.0 | 0.5 | 0.5 |
| $\rho_f$ (%)[11] | 1.9 | 1.3 | 0.8 | 0.60 | 1.9 | 0.7 | 0.5 | 0.5 | 0.52 | 1.8 | 0.5 | 0.5 | 0.5 |
| $\rho_w$(%)[12] | 1.2 | 0.25 | | 0.25 | 0.25 | | | | 0.25 | 0.25 | | | |
| $R_g$[13] | 1.7 | 2.6 | 4.2 | 4.0 | 1.4 | 2.4 | 3.1 | 4.3 | 4.4 | 1.4 | 2.1 | 2.4 | 4.1 |

[1]cantilever wall length, [2]sum of flange widths, [3]sum of web widths, [4]thickness of flange, [5]wall total cross sectional area, [6]gross moment of inertia, [7]mass per floor, [8]fundamental period corresponding to $E_cI_g$, [9]axial compression stress at base, [10]flange reinforcement ratio at base, [11]flange reinforcement ratio at mid-height, [12]web reinforcement ratio, [13]ratio of elastic bending moment demand (calculated using $E_c I_g$) to nominal flexural strength.

## 3. ANALYTICAL MODEL FOR CONCRETE CANTILEVER SHEAR WALLS

Nonlinear response history analysis was performed using a specially developed hysteretic bending moment – curvature relationship implemented into computer program OpenSees (OpenSees 2008). The hysteretic model features a trilinear backbone curve and incorporates stiffness degradation and residual curvatures similar to what was observed in large-scale tests of concrete shear walls (Adebar et al., 2007; Thomsen and Wallace, 1995). The trilinear backbone curve developed by Adebar and Ibrahim (2002) was extended into a hysteretic bending moment - curvature relationship (see Fig. 1).

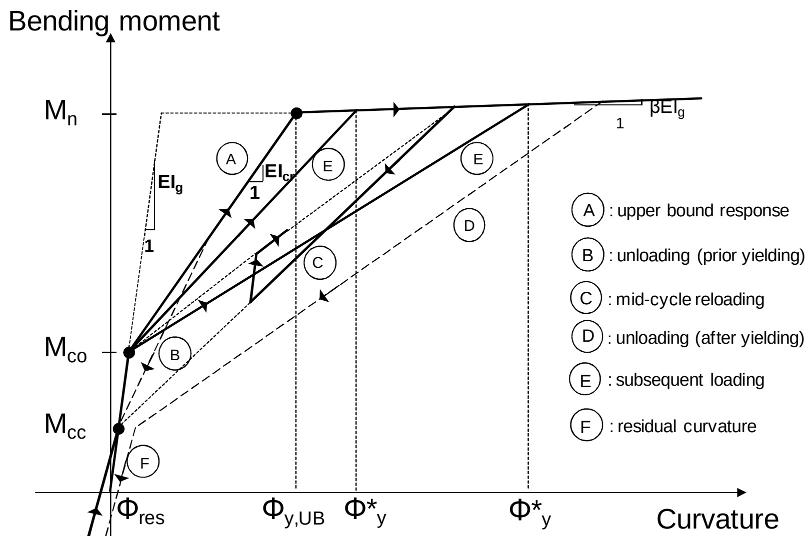


**Figure 1.** Trilinear bending moment – curvature relationship used for nonlinear response history analysis of cantilever walls.

The trilinear hysteretic model can be fully defined by the knowing the following parameters: $E_cI_g$ = uncracked flexural rigidity, $M_{co}$ = bending moment at crack opening, $M_n$ = flexural bending moment capacity, $\phi_y$ = yield curvature and $\beta$ = ratio of post-yield stiffness to initial stiffness, and $M_{cc}$ = bending moment at crack closing. Further details and validation of the trilinear bending moment – curvature model for cantilever shear walls is presented by Dezhdar (2012).

The parameters that define the trilinear hysteretic model were computed at each level considering the axial compression force and percentage of longitudinal reinforcement. A force element was defined at each floor level to model the spread of plasticity over the height. The base of the wall was assumed to be fixed and shear deformations were assumed to be zero for the analysis presented here; however additional studies were done to examine the influence of these on the building response (Dezhdar, 2012). Rayleigh damping was assumed with mass proportional and initial stiffness matrixes. A damping ratio of 3% was assigned for the first and third modes.

## 4. GROUND MOTIONS

As ground motions plays such an important role in the results that are obtained from nonlinear response history analysis, an extensive study was done to investigate different methods for selecting and scaling ground motions. Traditionally, ground motions are selected based on the magnitude and distance of a potential earthquake happening at the site as well as source mechanism and site soil condition. The ground motions are then scaled to the uniform hazard spectrum (UHS). Recently, Baker and Cornell (2006) introduced conditional mean spectrum (CMS) as an alternative target spectrum. The CMS accounts for the correlation between spectral accelerations at various periods. CMS is a more realistic scenario than UHS since the UHS is an envelope of spectral accelerations at all periods.

Eighty ground motions selected from the PEER Next Generation Attenuation (NGA) strong motion database (PEER 2010) were scaled to the UHS. For the buildings with fundamental periods of 1.0, 2.0, 3.0, 4.0, and 5.0 seconds, the number of ground motions were reduced to 80, 62, 53, 40, and 35 so that the mean spectrum matches the UHS over a wide range of periods. These ground motions are referred to as

SOR for “scaled over range.” Forty ground motions were spectrum matched to the UHS using computer program SYNTH (Naumoski 2001) and are referred to as SM.

For scaling to the CMS, nine periods were considered as conditioning periods for 10, 30, and 50 story shear walls: $T_2$ = 0.15 s, $T_1$ = 1.0 s, 1.5$T_1$ = 1.5 s and 2.0$T_1$ = 2.0 s for the 10 story walls, $T_3$ = 0.15 s, $T_2$ = 0.50 s, $T_1$ = 3.0 s and 5.0 s for the 30 story walls, and $T_3$ = 0.28 s, $T_2$ = 0.80 s and $T_1$ = 5.0 s for the 50 story walls. These are modal periods with a total mass equal to 90% of the total mass as well as periods representing the first mode period elongation due to nonlinear behavior. Maximum value for conditioning period is limited to 5.0 seconds since the simplified correlation model (Baker and Cornell 2006) was employed to compute the CMS. The Jayaram et al. (2011) approach was used to select forty ground motions for each conditioning period. Figure 2 shows an example of the target spectrum for 30 story walls with $T_1$ = 3.0 s.

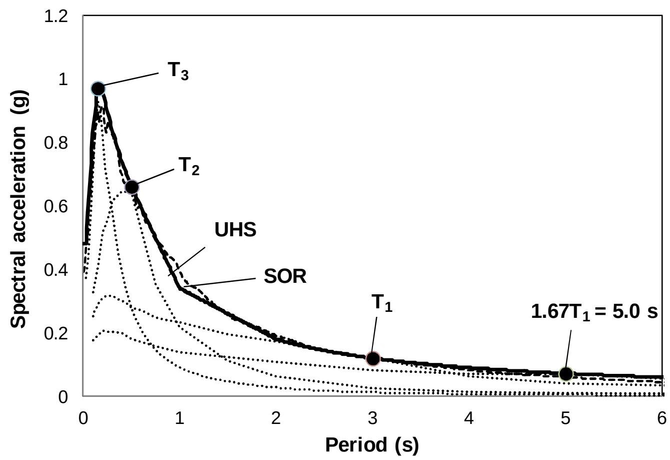


**Figure 2.** Comparison of UHS with mean spectrum for SOR and CMS computed at different conditioning periods.

## 5. ROOF DISPLACEMENT DEMANDS

Table 2 compares mean roof displacement demand determined from nonlinear response history analysis using different sets of ground motions. The CMS envelope associated with the largest responses are denoted as CMS-E. The mean roof displacements associated with the CMS-E were found to be between 90 and 100% of the mean roof displacement determined using the SM ground motions. It was also observed that mean roof displacements from SOR are between 90 and 110% of the mean results from SM ground motions.

Mean roof displacement from nonlinear response history analysis using SOR ground motions were used to determine effective stiffness of concrete shear walls. Appropriate effective stiffness values were determined such that the roof displacement from response spectrum analysis (RSA) matches the mean roof displacement from the time history analysis. A stiffness reduction factor of 1.0 was assumed as the first guess and it was reduced iteratively until the best match for roof displacement was achieved.

**Table 2.** Mean roof displacement demand using different sets of ground motions.

| Mean Roof displacement (m) | | | | | | | |
|---|---|---|---|---|---|---|---|
| | | | | | CMS | | |
| **Wall** | **$R_g$** | **SM** | **SOR** | **CMS-E** | **$2T_1$** | **$1.5T_1$** | **$T_1$** |
| 10 story | 1.7 | 0.119 | 0.117 | 0.114 | 0.088 | 0.111 | **0.114** |
| | 2.6 | 0.134 | 0.134 | 0.126 | 0.093 | **0.126** | 0.124 |
| | 4.2 | 0.190 | 0.183 | 0.169 | 0.138 | **0.169** | 0.138 |
| 30 story | 1.4 | 0.437 | 0.434 | 0.431 | - | 0.331 | **0.431** |
| | 2.4 | 0.561 | 0.523 | 0.520 | - | 0.457 | **0.520** |
| | 3.1 | 0.651 | 0.565 | 0.586 | - | 0.531 | **0.586** |
| | 4.3 | 0.641 | 0.593 | 0.592 | - | 0.518 | **0.592** |
| 50 story | 1.4 | 0.710 | 0.746 | 0.656 | - | - | **0.656** |
| | 2.1 | 0.810 | 0.818 | 0.771 | - | - | **0.771** |
| | 2.4 | 0.801 | 0.820 | 0.731 | - | - | **0.731** |
| | 4.1 | 0.690 | 0.754 | 0.635 | - | - | **0.635** |

The effective flexural stiffness of a concrete shear wall is normally thought to increase with the level of axial compression applied to the wall because compression increases the bending moment to cause flexural cracking. The results of the current study indicate the most important parameter that influences effective flexural stiffness is the ratio of elastic bending moment demand to strength of wall, and that generally the effective stiffness of concrete walls do not reduce below about 50% of the stiffness of an uncracked wall. Figure 3 shows the variation of stiffness reduction factors for the thirteen different buildings as a function of $R_e$, which is defined as the ratio of elastic bending moment demand (at base) calculated using $EI_e$ to the wall nominal flexural strength $M_n$. Note that the elastic demand to capacity ratios determined using $EI_e$ are smaller than the same ratios determined using $EI_g$ (see Table 3).

The axial compression stress ratio was found to have much less influence on the effective stiffness of concrete walls than previously thought, and for walls with a constant ratio of elastic demand to strength $R$, the wall with the highest axial compression stress ratio actually has the lowest effective stiffness because that wall has proportionally less vertical reinforcement and thus less hysteretic damping. Further details are given by Dezhdar and Adebar (2010).

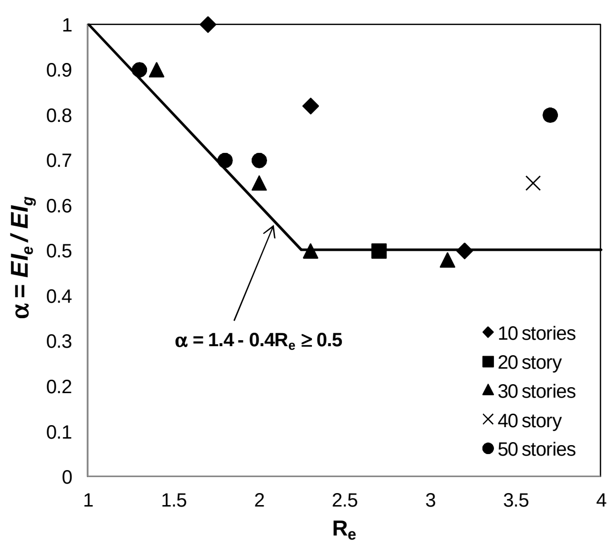


**Figure 3.** Variation of effective stiffness of cantilever walls as a function of the ratio $R_e$ of elastic bending moment demand at wall base to nominal bending moment capacity.

**Table 3.** Elastic bending moment demand to nominal capacity ratios corresponding to gross flexural stiffness ($R_g$) and effective stiffness ($R_e$).

| No. Stories | 10 | | | 20 | 30 | | | | 40 | 50 | | | |
|---|---|---|---|---|---|---|---|---|---|---|---|---|---|
| $P/f_c'A_g$ (%) | 5.9 | | | 8.7 | 10.1 | | | 6.1 | 6.2 | 12.7 | | | 6.2 |
| $R_g$ | 1.7 | 2.6 | 4.2 | 4.0 | 1.4 | 2.4 | 3.1 | 4.3 | 4.4 | 1.4 | 2.1 | 2.4 | 4.1 |
| $R_e$ | 1.7 | 2.3 | 3.3 | 2.7 | 1.3 | 2.0 | 2.3 | 3.1 | 3.6 | 1.3 | 1.8 | 2.0 | 3.7 |
| $EI_e/EI_g$ | 1.00 | 0.82 | 0.50 | 0.50 | 0.90 | 0.65 | 0.50 | 0.50 | 0.65 | 0.90 | 0.70 | 0.70 | 0.80 |

## 6. INTERSTORY DRIFT RATIOS

Interstory drifts of shear walls strongly influence deformation demands on gravity load columns connected to shear walls. For example, larger interstory drifts cause larger rotational demands on slab-column connections and this increases the likelihood of a punching shear failure of slabs.

Time history results of interstory drift ratio at the roof and at the mid-height showed that these are well correlated to the roof displacement demand. That is, the roof and mid-height interstory drift demands at the instant of maximum roof displacement are very similar to the corresponding maximum values. Consequently, roof and mid-height interstory drift demands can be expressed as a function of global drift ratio $\Delta_t /h_w$, which is the ratio of roof displacement demand to the wall height. It was observed that interstory drift at the roof and at the mid-height is relatively independent of the ratio $R$ of elastic bending moment demand at base to nominal capacity.

Figure 4(a) compares the interstory drift profiles from nonlinear response history analysis with the proposed envelopes for the 30 story wall with $R_e$ = 3.1. RSA can be used to make a good estimate of mean roof displacement, but it underestimates interstory drifts at lower floors. It is interesting to note that μ and μ+σ interstory drifts from SOR and CMS-E ground motions were found to be very similar. Figure 4(b) presents the proposed simplified envelope of interstory drift demands over the height. To estimate the mean (μ) interstory drifts, the parameters $A_r$, $A_m$, $A_r$ shall be taken equal to 1.6, 1.3, 0.7, while to estimate the mean plus one standard deviation (μ+σ) interstory drifts, these same parameters become 2.2, 1.8, 1.0.

(a) (b)

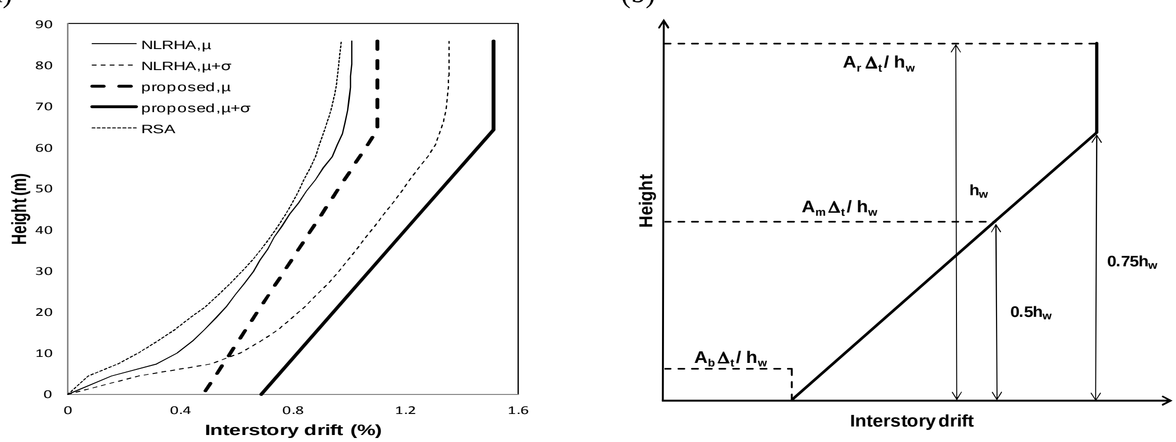


**Figure 4.** (a) Envelopes of interstory drifts for 30-story wall with $R_e$ = 3.1, and (b) proposed general interstory drift envelopes.

## 7. CURVATURE DEMANDS

Wall curvature demands influence the maximum compression strain demands in concrete and maximum tension strain demands in vertical reinforcement. Thus the displacement capacity of a concrete shear wall is directly linked to the maximum curvatures that result from wall displacements. Cantilever shear walls have traditionally been design for yielding only at the base due primarily to first mode bending moments; however many studies have shown that large bending moments also occur near mid-height due to higher mode (primarily second mode) bending moments.

Figure 5 presents the mean curvature demand envelopes for the cantilever walls in the four different 50-story buildings. The base curvature demand increases significantly as the flexural strength of the wall is reduced. The maximum mid-height curvature is less sensitive to the flexural strength of the walls. For example, the maximum mid-height curvature for 50-story walls with $R_e$ equal to 1.8 and 3.7 are identical (0.133 rad/km for $R_e$ = 1.8 versus 0.132 rad/km for $R_e$ = 3.7). At the location that the maximum curvatures occur, the nominal flexural strength of the $R_e$ = 1.8 wall is 1.5 times the strength of the $R_e$ = 3.7 wall.

Table 4 presents the mean and mean plus one standard deviation of mid-height curvature demands from nonlinear response history analysis. The maximum variation of strain across the wall at mid-height, which is equal to the product of the curvature times the wall length, varies from 0.0014 to 0.0023 (average value of 0.0019) for the mean curvature demands and from 0.0025 to 0.0042 (average of 0.0034) for the mean plus one standard deviation demands. These curvature demands are all very small and thus there is no need to try and prevent flexural yielding of cantilever shear walls near mid-height by trying to increase the flexural capacity of the walls as has been proposed by some researchers.

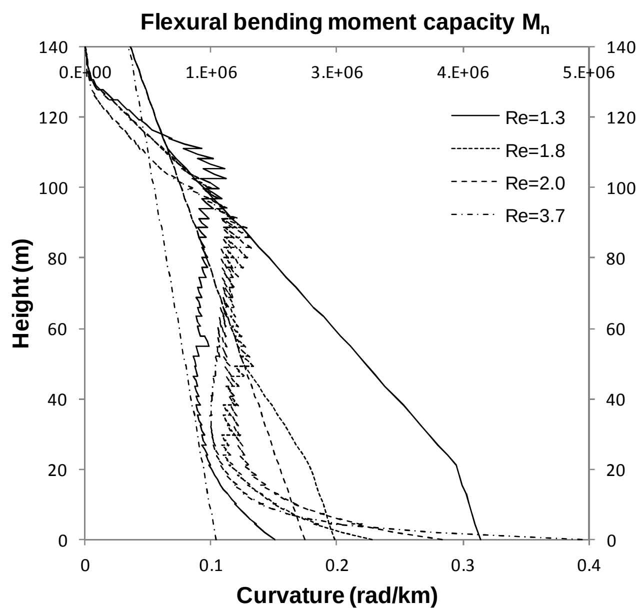


**Figure 5.** Variation of mean curvature demand envelopes for four different 50-story cantilever walls with different ratios $R_e$ of elastic bending moment demand (determined using $EI_e$) to nominal bending moment capacity. Also shown are the nominal bending moment capacity envelopes.

**Table 4.** Mean (μ) and mean plus one standard deviation (μ+σ) results for mid-height curvature times wall length, $\phi_{mid}.l_w$.

| | No. Stories | 10 | | | 20 | 30 | | | | 40 | 50 | | | | |
|---|---|---|---|---|---|---|---|---|---|---|---|---|---|---|---|
| | $R_e$ | 1.7 | 2.3 | 3.3 | 2.7 | 1.3 | 2.0 | 2.3 | 3.1 | 3.6 | 1.3 | 1.8 | 2.0 | 3.7 | Average |
| $\phi_{mid}.l_w$ | μ (x $10^3$) | 1.8 | 2.0 | 2.1 | 2.3 | 1.4 | 2.0 | 1.9 | 2.1 | 1.8 | 1.5 | 1.8 | 1.9 | 2.3 | **1.9** |
| | μ+σ (x $10^3$) | 3.5 | 3.7 | 3.7 | 4.2 | 2.7 | 3.9 | 3.2 | 3.7 | 3.3 | 2.7 | 2.9 | 2.5 | 4.0 | **3.4** |

## 8. SHEAR FORCE DEMANDS

Accurately estimating shear force demand is of particular importance in the seismic design of cantilever shear walls in order to ensure these structures will have a ductile response. Due to the influence of higher modes, the shear force demands from nonlinear response history analysis are considerably larger than those from linear analysis. The difference between shear force demands from the two approaches is often called the dynamic shear amplification.

Figure 6 compares mean shear force profiles for three walls using the SOR ground motions as well as ground motions matched and scaled to the CMS at different conditioning periods. For the 10 story wall, the CMS at $T_2$ and 1.5$T_1$ defines the envelope at the base and mid-height, respectively. Mean shear forces from CMS ground motions are 14 and 13% lower than those from the SOR ground motions at the base and mid-height, respectively. Also, changing conditioning period from $T_2$ to 1.5$T_2$ did not change the mean shear force envelope, which indicates that the elongation of higher mode has no effect on shear force distribution over the height for this shear wall.

For the 50-story wall, the CMS at 2$T_3$ defines the shear force envelope over the elevation range from 70 to 90 m. The mean shear force from this conditioning period is very similar to those determined using SOR ground motion, which indicates that high mid-height shear forces for the 50 story wall with $R$ = 2.0 are derived by the elongation of the third mode period. It should be mentioned that the mean shear force from $T_3$ defines the shear force envelope at the base (69900 kN), which is approximately 9% lower than that using the SOR ground motions.

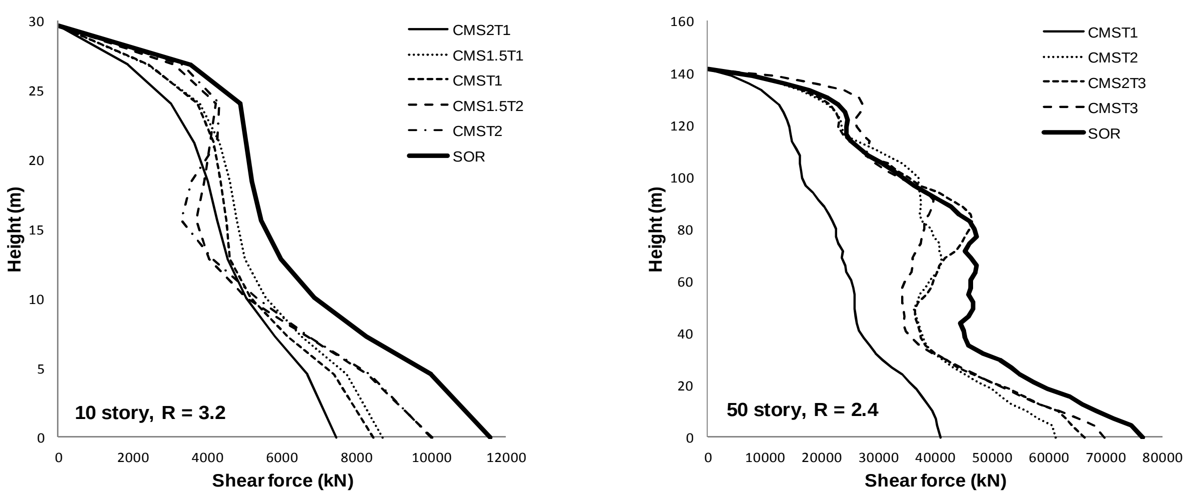


**Figure 6.** Mean shear force envelopes from different suites of ground motions for 10 and 50 story buildings.

In design, the base shear force determined using response spectrum analysis is reduced by the same ratio that the elastic bending moments are reduced to account for flexural ductility of the structure. The shear amplification is the amount these design shear forces (reduced from the elastic analysis) need to be increased again. In order to establish a simple model for shear amplification, the mean base shear force from nonlinear response history analysis was compared with the base shear force determined from response spectrum analysis for fixed-base cantilever walls. Elastic modes 1 to 4 and an effective stiffness of $0.5EI_g$ were used to compute elastic bending moments and shear forces. The modal forces were combined using the CQC method.

Figure 7 summarizes the shear amplification factors required for the 13 different buildings, which generally vary from 1.0 to 2.0 as the ratio of elastic bending moment at the base corresponding to $0.5EI_g$ to wall flexural capacity $M_n$ increases. For the 10-story walls, the shear amplification factor varies from 1.3 to 1.7, while the largest shear amplification factor for the 20, 30, and 50-story walls is 1.9. Also shown in Figure 7 is the proposed equation for calculating the shear amplification factors for cantilever shear walls based on elastic shear forces and bending moments determined using $0.5EI_g$.

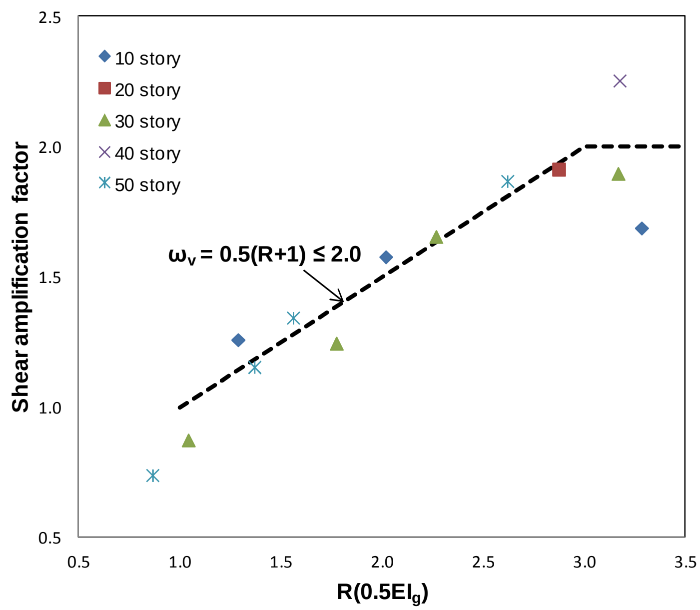


**Figure 7.** Shear amplification factor – defined as amount elastic shear forces reduced by $R$ need to be increased based on nonlinear analysis, where $R$ is ratio of elastic bending moment demand to nominal flexural capacity and all elastic forces determined from RSA using $0.5EI_g$.

## 9. CONCLUSIONS

Nonlinear response history analysis using 13 different buildings and many different ground motions was undertaken in order to develop simplified models for predicting seismic demands on cantilever shear wall buildings from linear dynamic (response spectrum) analysis. The main conclusions from this study are: (1) the effective flexural rigidity of cantilever shear walls that should be used to obtain an accurate estimate of maximum roof displacement reduces from 1.0 to about 0.5 as the ratio of elastic bending moment demand to flexural capacity of the wall increases. (2) A simplified envelope of interstory drifts is proposed, which can be used to estimate seismic deformation demands on gravity-load frame members such as rotations in slab-column connections and curvature demands on gravity-load columns (Adebar et al., 2012). (3) The maximum mid-height curvature demands on cantilever shear walls are relatively small and there is no reason to increase the strength of cantilever shear walls to prevent mid-height yielding or to provide excessive ductility requirements at the wall mid-height. (4) The shear amplification factor is the amount that design base shear force – reduced from elastic analysis by the same ratio that elastic bending moments are reduced to account for flexural ductility – need to be increased. This amplification factor was found to be independent of the building height and to have a maximum value of 2.0.

## REFERENCES


Adebar, P., Bazargany, P. and Chin, H. (2012). "Seismic Demands on Gravity-Load Columns in Shear Wall Buildings," 15th World Conference on Earthquake Engineering, Lisbon, Sept., 10 pp.

Adebar, P., and Ibrahim, A.M.M. (2002). Simple nonlinear flexural model for concrete shear walls. *Earthquake Spectra*. 18:3, 407-426.

Adebar, P., Ibrahim, A.M.M., and Bryson, M. (2007). Test of high-rise core wall: effective stiffness for seismic analysis. *ACI Structural Journal*. 104:5, 549-559.

Baker, J. W., and Cornell, C. A. (2006). Spectral shape, epsilon, and record selection. *Earthquake Engineering and Structural Dynamics*. 35:9, 1077-1095.

CSA Committee A23.3 (2004). Design of Concrete Structures - A National Standard of Canada, Canadian Standards Association, Rexdale, Canada.

Dezhdar, E. (2012). Seismic Response of Cantilever Concrete Shear Wall. *PhD thesis*. The University of British Columbia, Vancouver, Canada.

Dezhdar, E., and Adebar, P. (2010). Effective stiffness of high-rise cantilever shear walls. *Proceedings of 9th U.S National and 10th Canadian Conference on Earthquake Engineering*, Toronto, Ontario.

Jayaram, N., Lin, T., and Baker, J.W. (2011). A computationally efficient ground motion selection algorithm for matching a target response spectrum mean and variance. *Earthquake Spectra*. 27:3, 797-815.

Naumoski, N. D. (2001). Program SYNTH Generation of Artificial Accelerograms Compatible with a Target Spectrum. *Computer Program and Supporting Documentation*. Carleton University, Ottawa, Canada.

Pacific Earthquake Engineering Research Center (PEER). 2008. Open System for Earthquake Engineering Simulation (OpenSees). *Computer Program and Supporting Documentation*. University of California, Berkeley.

Pacific Earthquake Engineering Research Center (PEER). 2010. PEER NGA database flatfile.

Thomsen, J., and Wallace, J.W. (1995). Displacement-based design of reinforced concrete structural walls: an experimental investigation of walls with rectangular and T-shaped cross sections. *MASc thesis*. Clarkson University, Postdam, N.Y.